Technical University of Denmark

DTU

340 nm pulsed UV LED system for europium-based time-resolved fluorescence detection of immunoassays

Rodenko, Olga; Fodgaard, Henrik; Tidemand-Lichtenberg, Peter; Petersen, Paul Michael; Pedersen, Christian

Published in:
Optics Express

Link to article, DOI:
10.1364/OE.24.022135

Publication date:
2016

Document Version
Publisher's PDF, also known as Version of record

Link back to DTU Orbit

DTU Library
Technical Information Center of Denmark

340 nm pulsed UV LED system for europium-based time-resolved fluorescence detection of immunoassays

OLGA RODENKO,[1,2*] HENRIK FODGAARD,[2] PETER TIDEMAND-LICHTENBERG,[1] PAUL MICHAEL PETERSEN,[1] AND CHRISTIAN PEDERSEN[1]

[1]*Technical University of Denmark, Frederiksborgvej 399, 4000 Roskilde, Denmark*
[2]*Radiometer Medical ApS, Aakandevej 21, 2700 Broenshoej, Denmark*
*olro@fotonik.dtu.dk

Abstract: We report on the design, development and investigation of an optical system based on UV light emitting diode (LED) excitation at 340 nm for time-resolved fluorescence detection of immunoassays. The system was tested to measure cardiac marker Troponin I with a concentration of 200 ng/L in immunoassay. The signal-to-noise ratio was comparable to state-of-the-art Xenon flash lamp based unit with equal excitation energy and without overdriving the LED. We performed a comparative study of the flash lamp and the LED based system and discussed temporal, spatial, and spectral features of the LED excitation for time-resolved fluorimetry. Optimization of the suggested key parameters of the LED promises significant increase of the signal-to-noise ratio and hence of the sensitivity of immunoassay systems.

References and links

1. E. Soini and H. Kojola, "Time-resolved fluorometer for lanthanide chelates--a new generation of nonisotopic immunoassays," Clin. Chem. **29**(1), 65–68 (1983).
2. G. Marriott, R. M. Clegg, D. J. Arndt-Jovin, and T. M. Jovin, "Time resolved imaging microscopy. Phosphorescence and delayed fluorescence imaging," Biophys. J. **60**(6), 1374–1387 (1991).
3. E. J. Hennink, R. de Haas, N. P. Verwoerd, and H. J. Tanke, "Evaluation of a time-resolved fluorescence microscope using a phosphorescent pt-porphine model system," Cytometry **24**(4), 312–320 (1996).
4. E. P. Diamandis and T. K. Christopoulos, "Europium Chelate Labels in Time-Resolved Fluorescence immunoassays and DNA hybridization assays," Anal. Chem. **62**(22), 1149A–1157A (1990).
5. L. Seveus, M. Väisälä, S. Syrjänen, M. Sandberg, A. Kuusisto, R. Harju, J. Salo, I. Hemmilä, H. Kojola, and E. Soini, "Time-resolved fluorescence imaging of europium chelate label in immunohistochemistry and in situ hybridization," Cytometry **13**(4), 329–338 (1992).
6. R. Connally, D. Veal, and J. Piper, "Flash lamp-excited time-resolved fluorescence microscope suppresses autofluorescence in water concentrates to deliver an 11-fold increase in signal-to-noise ratio," J. Biomed. Opt. **9**(4), 725–734 (2004).
7. E. Reichstein, Y. Shami, M. Ramjeesingh, and E. P. Diamandis, "Laser-excited time-resolved solid-phase fluoroimmunoassays with the new europium chelate 4,7-Bis(chlorosulfophenyl)-1,10-phenanthroline-2,9-dicarboxylic acid as label," Anal. Chem. **60**(10), 1069–1074 (1988).
8. D. Jin, R. Connally, and J. Piper, "Long-lived visible luminescence of UV LEDs and impact on LED excited time-resolved fluorescence applications," J. Phys. D Appl. Phys. **39**(3), 461–465 (2006).
9. R. Connally, D. Jin, and J. Piper, "High intensity solid-state UV source for time-gated luminescence microscopy," Cytometry A **69**(9), 1020–1027 (2006).
10. N. Gahlaut and L. W. Miller, "Time-resolved microscopy for imaging lanthanide luminescence in living cells," Cytometry A **77**(12), 1113–1125 (2010).
11. K. Davitt, Y.-K. Song, W. Patterson Iii, A. Nurmikko, M. Gherasimova, J. Han, Y.-L. Pan, and R. Chang, "290 and 340 nm UV LED arrays for fluorescence detection from single airborne particles," Opt. Express **13**(23), 9548–9555 (2005).
12. H. Peng, E. Makarona, Y. He, Y.-K. Song, A. V. Nurmikko, J. Su, Z. Ren, M. Gherasimova, S.-R. Jeon, G. Cui, and J. Han, "Ultraviolet light-emitting diodes operating in the 340 nm wavelength range and application to time-resolved fluorescence spectroscopy," Appl. Phys. Lett. **85**(8), 1436–1438 (2004).
13. P. von Lode, J. Rosenberg, K. Pettersson, and H. Takalo, "A europium chelate for quantitative point-of-care immunoassays using direct surface measurement," Anal. Chem. **75**(13), 3193–3201 (2003).

14. N. K. Seitzinger, K. D. Hughes, and F. E. Lytle, "Optimization of signal-to-noise ratios in time-filtered fluorescence detection," Anal. Chem. **61**(23), 2611–2615 (1989).
15. M. Latva, H. Takalo, V.-M. Mukkala, C. Matachescu, J. C. Rodriguez-Ubis, and J. Kankare, "Correlation between the lowest triplet state energy level of the ligand and lanthanide(III) luminescence quantum yield," J. Lumin. **75**(2), 149–169 (1997).

1. Introduction

Time-resolved fluorescence is a powerful tool that has been used in immunoassays detection to suppress short-lived background fluorescence and allow for high sensitivity [1]. It relies on employing high-fluorescent fluorophores with long fluorescence lifetime and light sources emitting excitation pulses terminating prior to the gated measurement. Moreover, the fall time of the excitation pulse has to be shorter than the delay between the excitation and detection [2,3]. Time-gated fluorescence detection delayed by microseconds exhibits improved signal-to-background ratio (S/B) and often improved signal-to-noise ratio (SNR) compared to steady-state measurements as it reduces interference from unwanted fluorophores having a fluorescence lifetime typically in the range of nanoseconds [1]. Many fluorophores with long fluorescence lifetime belong to the group of lanthanides. Europium Eu^{3+} is a lanthanide ion which has been widely used as a marker in time-resolved fluorescence instruments due to its large Stokes shift and long fluorescence lifetime (μs-ms) [4]. Europium chelates are excited in the UV-A region and emit fluorescence with an emission peak at 616 nm with a FWHM of 10-20 nm. As an excitation light source, Xenon flash lamps have been widely used for this application [5,6]. One of the main concerns using a flash lamp is its long trailing afterglow lasting for hundreds of microseconds that reduces SNR [6]. As an alternative excitation light source, nitrogen lasers have been implemented but they are bulky, expensive, and operate at low repetition frequencies [7].

UV LEDs have emerged as a new attractive light source for time-resolved excitation shown in the following. LEDs have smaller footprint, better heat dissipation, higher wall-plug efficiency and higher operational stability compared to Xenon flash lamps. They are compact and cost-effective. Their narrowband emission spectrum allows better matching to particular peaks of the europium chelates excitation spectra. Moreover, LEDs exhibit no significant afterglow when compared to flash lamps [8]. Output power and temporal parameters of LEDs can be controlled easily by simple electronics in contrast to flash lamp electronics. The technological advancement of LEDs has already resulted in the development of the lanthanide chelates based time-resolved systems using LED excitation at 365 nm [9]. A 100 mW single LED at 365 nm with pulse duration of 101 μs and a gate delay of 5 μs was employed for excitation in time-gated luminescence microscopy [9]. LEDs at 365 nm were also used in a time-resolved luminescence microscope for pulsed epi-illumination [10]. 340 nm LED has until now been hampered by limited power [11]. Closest prior art has been LEDs at 340 nm with output power up to 1 mW and dimension <100 μm in diameter which were employed in fluorescence lifetime measurements [12].

LEDs at 340 nm with pulse energies comparable to flash lamps have only recently become available and to our knowledge, this is the first report of the design, development and characterization of a single emitter, 340 nm LED based time-resolved fluorescence system for immunoassays detection. The obtained pulse energies were up to 5 μJ, with LED output power up to 50 mW, which is comparable to the typical flash lamp and as required by our application. We performed a comparative study of this high power LED with the Xenon flash lamp and discuss spatial, spectral and temporal features of LED illumination when used for time-resolved fluorescence measurements.

2. Optical design

The optical system is a reflection-type fluorescence system and includes two subsystems, excitation light path and detection light path, see Fig. 1. In the first subsystem, light is collected from a Lambertian emitter with an area of 1x1 mm^2 (SMD LED YL-6363F-340nM

purchased from YesLED, Hong Kong) by an aspheric lens with a short focal length and high numerical aperture (NA). The next two plano-convex lenses and a biconvex lens form an image 50 mm away. All lenses are made of UV grade fused silica to ensure high transmission in the UV-A region and to minimize autofluorescence from the lens material. The magnification of the system is −5, limited by the object and image side numerical apertures. The image is formed in the bottom of the UV absorbing test cup which is made of polystyrene. The inner cup diameter is 6.7 mm and the cup side is 10.6 mm in height, thus limiting the acceptance angle of the image side to 17.5°. The excitation system is designed for maximum collection efficiency reaching 80%. If smaller magnification is needed, the first lens, f_1 needs to have a larger focal length and thus smaller object side NA, or alternatively, the last lens, f_4 needs to have shorter focal length, thus larger image side NA. The first option reduces the collection efficiency. The second option is not feasible due to the limited acceptance angle of the test cup and the mechanical requirement of a minimum distance between beam splitter and test cup. Thus, there is a trade-off between the magnification and collection efficiency when selecting the first lens, f_1. A dichroic beam splitter separates the excitation and detection light paths. Emitted fluorescence is collected by two aspheric PMMA lenses and focused on a photocathode of a photomultiplier tube (PMT) with a magnification of −1. The PMT has a photocathode effective area of 8x24 mm^2 and is configured for photon counting mode. Two bandpass filters in the excitation and detection systems ensure that only emitted fluorescence reaches the PMT. The reference photodiode is used to monitor the light source power.

Using commercial ray tracing software the image of the light source was modeled. The image is a square with 90% of the power encircled in a 5x5 mm^2 area, see Fig. 2(a). The obtained experimental image was in good agreement with model, as shown in Fig. 2(b). The low-intensity decaying edges are not observed experimentally due to limited dynamic range of the camera used. The LED image covers 71% of cup bottom area, which is three times larger than the flash lamp image. The exploited illumination area is limited by the PMT photocathode area and its field of view (FOV). The calculated FOV corresponds to a 5 mm diameter circle at the bottom of the cup, thus using a larger LED emitting area is not an advantage.
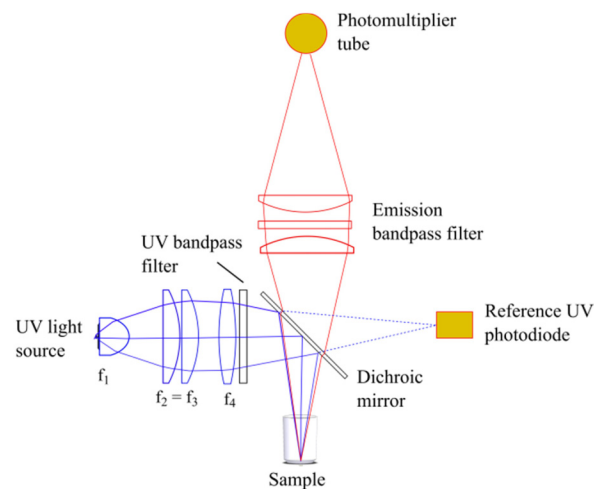

Fig. 1. Schematic layout of the optical system including excitation and detection light paths.

The Xenon flash lamp used in the current optical system has a lamp arc length of 1.5 mm. It is imaged with a magnification of −2 in the sample cup, see Fig. 2(c). Out of the broadband spectrum of the flash lamp (200–1100 nm) only 110 nm are spectrally selected for sample

excitation. The flash lamp is triggered by a FPGA with a repetition frequency of 250 Hz. The object side NA is smaller (<0.5) compared to the UV LED, thus the collection efficiency is smaller due to vignetting. Therefore, the overall efficiency is much smaller for the flash lamp.
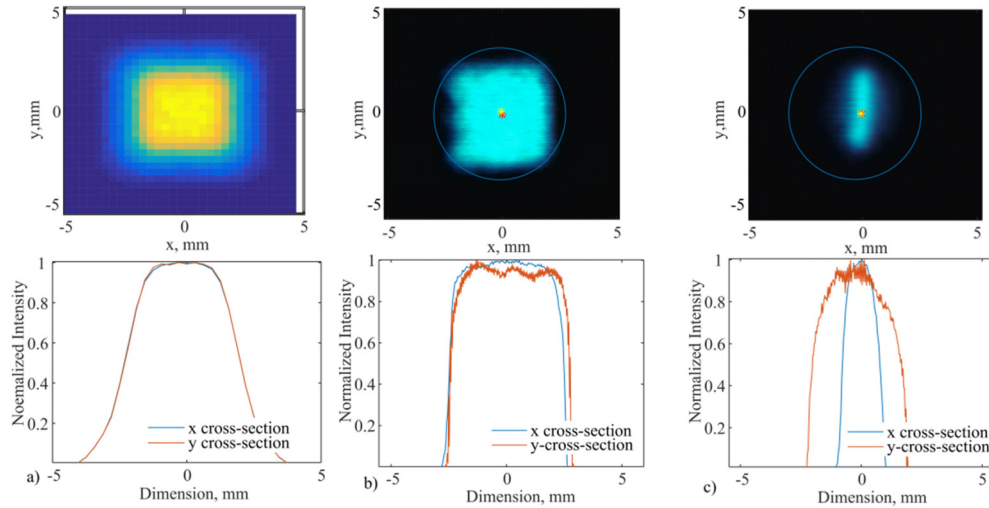

Fig. 2. Images formed in the test cup and its normalized intensity distribution, a) modeled LED image using commercial ray trace software; b) experimentally obtained LED image; the blue circle shows the boundary of cup bottom which is 6.7 mm in diameter; c) image of flash lamp arc (current light source). The illuminated area is 2x4 mm^2, thus three times smaller than that of the LED image.

3. Experimental characterization of the excitation system

The excitation spectrum of the Europium chelate has a peak at 325 nm with a FWHM of 64 nm, as shown in Fig. 3, left. The chelate structure and synthesis are described in [13]. It should be noted that different immunoassays can have slightly different excitation spectra with varying peak wavelength. Filters WG320 and Schott DUG11 transmit a 48 nm window of the flash lamp emission spectrum. The LED emission spectrum is centered at 343 nm with a FWHM of 10 nm. The LED emission spectrum has approximately 20% larger overlap with the europium chelate excitation spectrum than the filtered flash lamp. When increasing the LED current from 100 mA to 1 A in pulsed mode, no visual shift in peak wavelength was observed, see Fig. 3, right. Similar results were also reported in [12], thus indicating that UV LEDs are spectrally stable. The inset figure shows the normalized LED irradiance in a logarithmic scale. The light emission drops fast to 1% and 0.1% of peak emission at 372 nm and 404 nm, respectively.
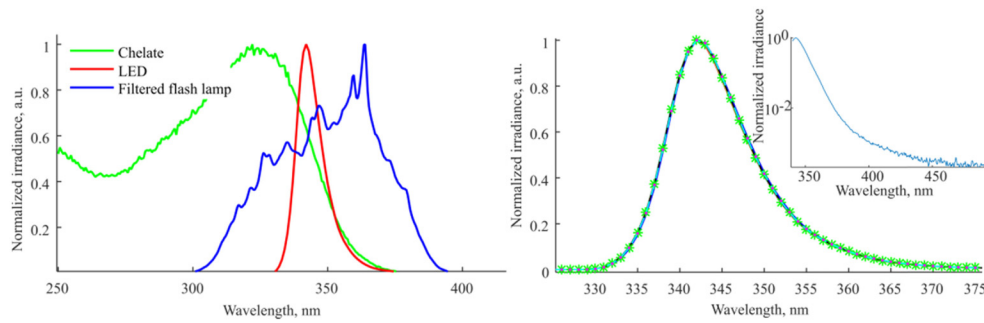
Fig. 3. Left: Normalized excitation spectrum of Europium chelate (green), normalized emission spectrum of the LED (red), and normalized emission spectrum of the filtered flash lamp (blue); right: normalized emission spectra of the LED for different LED currents ranging from 100 mA to 1 A (curves overlap); inset figure: normalized irradiance of the LED in logarithmic scale (chelate excitation spectrum courtesy: Radiometer Turku).
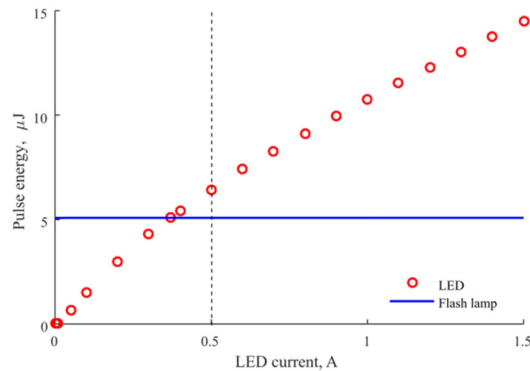

Fig. 4. Excitation pulse energy delivered to the cup vs. LED current. The pulse width is 200 µs and the duty cycle is 0.05. At a current of 370 mA, the delivered energy is equal to that of the currently used Xenon flash lamp. Energy levels up to 15 µJ are achieved when overdriving the LED three times above the specified maximum current of 500 mA (indicated by the dotted line).

With the current Xenon flash lamp, 5.1 µJ per pulse is delivered to the sample. The LED is capable of delivering up to 15 µJ at 1.5 A, which is still only three times above the maximum continuous wave current as specified with the dotted line in Fig. 4.

The LED is controlled by a LED driver, which is synchronized with the detection system. An FPGA controls both the excitation and detection systems using a trigger pulse train, which is transmitted to the LED driver via a pulse generator as demonstrated in Fig. 5, left. The LED pulse width is 200 µs which is three orders of magnitudes longer than the flash lamp pulse. The LED pulse width was chosen in order to deliver the same excitation energy as the flash lamp and to obtain a good SNR of the instrument without overdriving the LED. The LED pulse width can be longer thus increasing the excitation energy and improving the SNR, as long as the pulse terminates before the measurement. A delay of 8 µs between the trigger pulse and LED current pulse is observed and the fall time of the LED pulse is smaller than 3 µs. The flash lamp pulse is 200 ns and exhibits a long fall time of 400 ns (90% - 10%) relatively to its width. We have chosen a delay of 400 µs between the end of the excitation pulse and measurement window in order to match the typical timing parameter used for flash lamp excitation (required due to the flash lamp afterglow). This parameter can be optimized in the LED based excitation system. Reduced gate delay will increase the signal and improve the SNR, in contrast to the flash lamp based system.
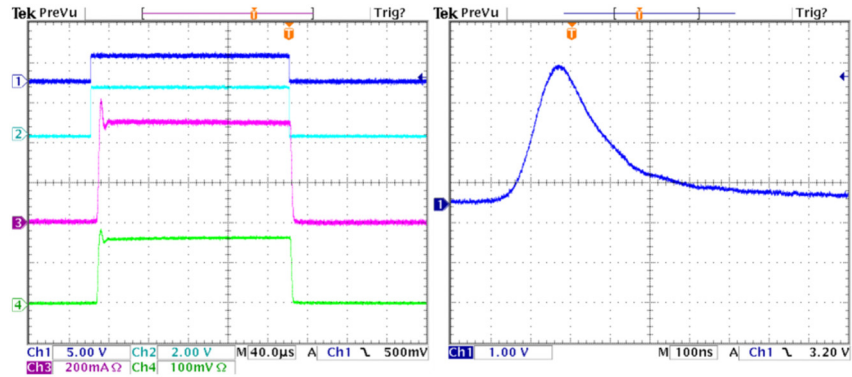
Fig. 5. Left: time response of the LED pulse triggering system; trigger pulse from the FPGA (dark blue); pulse generator (light blue); LED current pulse (magenta); and optical output (light green). The delay between the LED current pulse and the trigger is 8 μs and the LED fall time is below 3 μs; right: the Xenon flash lamp pulse showing a FWHM of 200 ns and a fall time of 400 ns.

The much longer LED pulse affects the excitation efficiency of chelates, but only slightly as discussed below. The LED pulse width is comparable to the fluorescence lifetime, whereas the flash lamp pulse is in the range of hundreds of nanoseconds. Therefore, the number of the fluorophore excited molecules at the end of the pulse is smaller in the first case. To demonstrate this, we propose a simple model. We write the population of excited molecules, N which is described by a simple rate equation:

$$\frac{dN}{dt} = R(t) - kN \tag{1}$$

$R(t)$ is pump rate proportional to excitation pulse peak power; k is decay rate constant of the fluorophore (inverse proportional to fluorescence lifetime τ). Solving Eq. (1), the number of molecules, N_0 when the excitation pulse is switched off is:

$$N_0 = \frac{R(t)}{k}\{1 - exp(-k \cdot \tau_p)\} \tag{2}$$

τ_p is the excitation pulse duration. Combining Eq. (1) and Eq. (2), the decay of excited molecules follows:

$$N(t) = R(t) \cdot \tau\{1 - exp(\frac{-\tau_p}{\tau})\} \cdot exp(\frac{-t}{\tau}) \tag{3}$$

Figure 6, left shows the number of excited molecules, N when illuminated by an excitation pulse of 200 ns and 200 μs respectively (blue and orange curve). N builds up exponentially during the pulse proportional to the excitation peak power and decays exponentially with the lifetime, τ when the pulse is switched off. This curve can also be obtained as a convolution of the excitation pulse and the fluorescence decay. The main conclusion is that a difference of three orders of magnitude in pulse widths only gives rise to a 10% decrease in the number of excited molecules, thus in the fluorescence signal, as shown in Fig. 6, right.
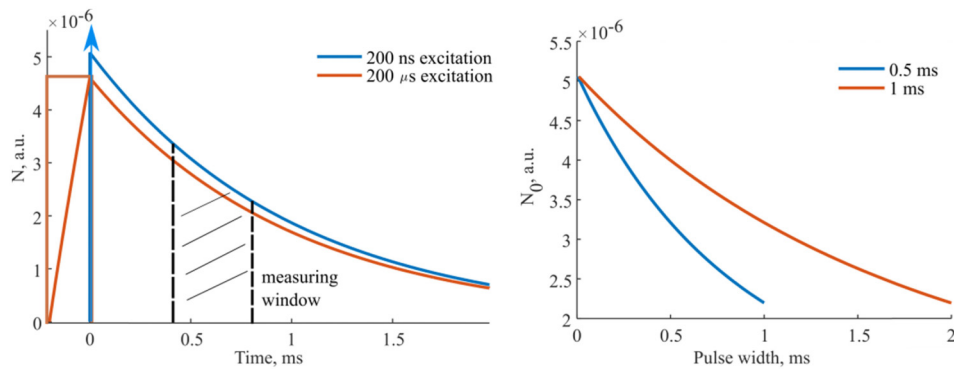
Fig. 6. Left: excitation pulse and number of excited molecules for a LED pulse of 200 µs (orange curve) and a 200 ns flash lamp pulse (blue curve); during the excitation pulse the number of excited molecules builds up exponentially and reaches the maximum value by the end of the pulse; then it decays exponentially with the decay rate constant, k, related to the europium lifetime of 1 ms. The number of excited molecules is 10% smaller for the longer excitation pulse; right: number of excited molecules vs. excitation pulse width with constant total energy for different fluorophore lifetimes.

4. Time-resolved detection of TnI protein in immunoassays

In order to test the full implication of substituting the flash lamp with a LED for excitation of europium chelates we performed a comparative study with the SNR as a key performance parameter encompassing all the different aspects as discussed in previous sections. The variation of the data is large due to the small sample size. It would require about 200 replicates to achieve a 95% confidence interval, [0.91·s; 1.08·s] for the standard deviation, s of the signal and background respectively. Therefore, a detailed investigation will be carried out later. The LED based system was tested for time-resolved fluorescence measurements of the cardiac marker, Troponin I (TnI). Test cups were investigated in the experiment with the TnI immunoassay using 200 ng/L (sample cups) and 0 ng/L (blank cups) concentrations with 15 replicates each, respectively. The experiment with the test cups was performed manually. Each cup was measured consecutively on a Xenon flash lamp and LED unit without rotation in the same cup holder. Each sample was exposed to 777 pulses of 5.1 µJ and with a repetition frequency of 250 Hz, corresponding to 1.27 mW average power. The measurements were performed without bleaching effects due to small exposed energy.

We define SNR similarly to [14] as the fluorescence signal, S corrected for the averaged background value, B and divided by an expression taking into account both signal and background variations (measured on blank cups, i.e. 0 ng/L): $SNR = \dfrac{\overline{S} - \overline{B}}{\sqrt{\sigma_S^2 + \sigma_B^2}}$. The SNR was

35.5 and 30.0 for the flash lamp based optical unit and the LED based optical unit, respectively (blue square and magenta rhomb in Fig. 7). The fluorescence response of the sample cups was 26% lower when excited with the LED unit, however the SNR decreased only by 15% for the LED compared to the flash lamp unit. Therefore, the SNR of the LED based unit was comparable to that of the flash lamp unit, with equal excitation energy. Several properties of the LED based system contribute to the reduced signal level: increased excitation pulse width and enlarged illumination area.
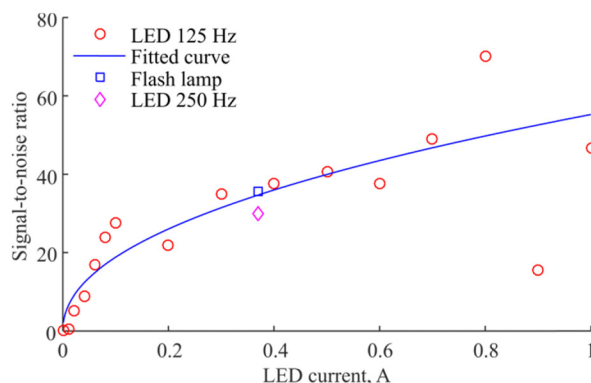
Fig. 7. Signal-to-noise ratio averaged for four cups vs. LED current for a TnI concentration of 200 ng/L; the SNR grows with the square root of excitation power (red circles); blue square and magenta rhomb show mean values for an experiment with 15 replicates for the flash lamp and LED based unit, respectively.

Four extra sample and blank cups were measured to demonstrate SNR dependence on the excitation energy. The LED was operated at the repetition frequency of 125 Hz however still with the same excitation energy so that it does not affect the signal, but only the measurements take longer time. Figure 7 shows SNR as a function of the LED current for a TnI concentration of 200 ng/L. The SNR was calculated for four replicates, shown as red circles and grows with the square root of LED current as expected (fitted blue curve). The behavior is explained by the Poisson distributed signal and noise in the system. The outliers at 0.8 and 0.9 A are presumably effects of the large variation of the data, as discussed above. The SNR can be improved by increasing the excitation energy with higher LED current and/or longer pulse width. Moreover, for constant excitation energy the SNR can be improved in different ways. Firstly, decreasing the excitation pulse width will enhance the signal however limited to a 10% improvement, see Fig. 6. Secondly, a better spectral overlap between chelate excitation spectrum and light source emission, will further improve the signal. Many lanthanide based chelates (such as Eu^{3+} or Tb^{3+}) have the excitation peak at 340 nm and therefore are a better match to the 340 nm LED [15]. An improvement by a factor of two is expected, if the light source emission peak matches the excitation peak. Thirdly, the delay time between the excitation and detection can be reduced in the LED based system, thus increasing the signal. Lastly, the roughly three times enlarged illumination area compared to the flash lamp system causes a signal reduction, if the chelates distribution in the cup is non-uniform and the chelates concentration is higher in the center of the cup than in the edges. It was observed that misalignment of the flash lamp image in the order of 1 mm in the instrument decreases the signal by up to 30% compared to a centered setup. Later experiments confirmed this observation. Optimum illumination area with the largest overlap with chelates distribution will result in higher fluorescence signal.

In order to demonstrate the impact of a LEDs narrower emission spectrum and its absence of afterglow, we introduce the signal-to-background ratio as the averaged signal to the averaged background as in [1]. The S/B was in our experiments improved by 18% (data not shown) when using LED illumination compared to the flash lamp system. Indeed preliminary experiments showed that the S/B was further improved when decreasing the illumination area. However, further investigation is needed.

Conclusion

For the first time to our knowledge, a time-resolved fluorescence system based on a 340 nm LED was successfully employed for immunoassays detection. The optical system was designed to collect up to 80% of LED light, emitted from the 1x1mm^2 Lambertian chip and

simultaneously be focused to an area of 5x5 mm^2 in the bottom of a test cup with a 6.7 mm diameter. The image area was three times larger than the image of the Xenon flash lamp, however still small enough to excite fluorescence efficiently and subsequently be imaged on the PMT photocathode. The LED was operated at 370 mA in pulsed mode. The LED pulse width was 200 μs and the pulse energy was 5.1 μJ when operated below the specified maximum current limit, comparable to the pulse energy from the Xenon flash lamp. A three orders of magnitude increase in pulse width of the LED excitation compared to the flash lamp was estimated to reduce the fluorescence signal by a mere 10% due to the long fluorescence lifetime of europium. The signal-to-background was improved significantly when excited by the LED, expectedly due to the absence of the flash lamps afterglow and narrower emission spectrum of the LED.

A test with real immunoassay samples of the cardiac marker TnI (200 ng/L), showed comparable SNR for the LED and Xenon flash lamp respectively for the same excitation pulse energy. A SNR of 35, equal to that of the flash lamp system, was obtained without overdriving the LED and can be further improved by increasing the LED current. Moreover, for constant excitation energy the SNR can be improved by reducing the illumination area, having shorter excitation pulse width and shorter delay time, and possibly better spectral match with the europium chelate excitation spectrum. Including the LEDs small footprint, cheaper price, better efficiency and heat dissipation, we conclude that UV LEDs will likely soon replace Xenon flash lamp excitation in immunoassays time-resolved detection systems based on long lifetime fluorophores.

Funding

Acknowledgments